
Enhancing Q-Learning with Large Language Model Heuristics

Xiefeng Wu
Wuhan University
wuxiefeng@whu.edu.cn

Abstract

Q-learning excels in learning from feedback within sequential decision-making tasks but requires extensive sampling for significant improvements. Although reward shaping is a powerful technique for enhancing learning efficiency, it can introduce biases that affect agent performance. Furthermore, potential-based reward shaping is constrained as it does not allow for reward modifications based on actions or terminal states, potentially limiting its effectiveness in complex environments. Additionally, large language models (LLMs) can achieve zero-shot learning, but this is generally limited to simpler tasks. They also exhibit low inference speeds and occasionally produce hallucinations. To address these issues, we propose **LLM-guided Q-learning** that employs LLMs as heuristic to aid in learning the Q-function for reinforcement learning. It combines the advantages of both technologies without introducing performance bias. Our theoretical analysis demonstrates that the LLM heuristic provides action-level guidance. Additionally, our architecture has the capability to convert the impact of hallucinations into exploration costs. Moreover, the converged Q function corresponds to the MDP optimal Q function. Experiment results demonstrated that our algorithm enables agents to avoid ineffective exploration, enhances sampling efficiency, and is well-suited for complex control tasks.

1 Introduction

Q-learning with function approximation is an effective algorithm for addressing sequential decision-making problems, initially proposed by [1]. In this approach, The Q-function is updated through Temporal Difference (TD) learning. This Q-learning process can be regarded as a form of supervised learning applied to a linked list dataset. In many popular Actor-Critic algorithms (A2C)[2, 3, 4], the Q-function is crucial in deriving policies, thereby implicitly guiding agent exploration and influencing sample collection strategies. However, employing the 2-norm to ensure the Q-function’s convergence to optimal values in expanding MDPs presents several challenges, including potential divergence[5] and high sampling demands.[3, 4]

Previous research has sought to enhance sample efficiency through reward shaping. [6, 7, 8] use count-based intrinsic bonuses $B_k(s)$ to encourage exploration. The bonus term measures the ‘novelty’ of a state s given the history of all transitions up to k . [9] uses the ranking of the trajectory of each sample as the reward heuristic and provides bias analysis. [10] uses a prior guess of the desired long-term return of states, adheres to potential-based reward design, and introduces a decay factor γ to prevent the impact of inaccuracy.

Using LLM/VLM as agents represents a viable approach for planning and control, although this method suffers from slow inference speeds and hallucinations. [11] employs an LLM as a world model, allowing it to directly output rewards and states. [12] utilizes an LLM to generate skill-based Python code, achieving autonomous exploration and skill expansion. LLMs as high level

controllers[13, 14, 15] can effectively translate the coarse-grained guidance of LLMs into fine-grained control. However, a significant drawback is that the meta-skill library requires manual expansion and has a theoretical upper limit.

Given the limitations of LLM/VLM agents and reward shaping, LLM-guided RL emerges as a promising research area. [16] utilizes the LLM’s action probability and a UCT term as heuristic components, specifically: $\hat{\pi}(a|h) \frac{\sqrt{N(h)}}{N(h,a)+1}$, to influence the Q value. [17] expands the observation input using an LLM and solely relies on the LLM’s environmental analysis as the reward function. [18] implements automated preference labeling through a VLM. These studies, while innovative in designing LLM-based reward heuristics, introduce performance errors and are susceptible to hallucinations.

To tackle these challenges, we propose a novel LLM-guided RL framework called **LLM-guided Q-learning** that introduces a heuristic term, \mathbf{h} , to the Q-function, expressed as: $\hat{\mathbf{q}} = \mathbf{q} + \mathbf{h}$. By employing the LLM generated heuristic term to modulate the values of the Q-function, we implicitly induce the desired policy. Contrary to potential-based reward shaping, which is constrained by inherent limitations, the design of Q-heuristics exhibits remarkable flexibility. This heuristic framework can universally incorporate guidance from a diverse array of sources, including linguistic inputs, visual data, corrections, entropy measurements, and domain-specific samples.

In our theoretical analysis, we demonstrate that the heuristic term can help reduce suboptimality and discuss the impact of hallucinations from the perspectives of overestimation and underestimation. We then prove that the reshaped Q function, $\hat{\mathbf{q}}$, maintains the same fixed-point for any Markov Decision Process (MDP), thereby ensuring it does not introduce bias into the agent’s performance. Finally, we provide the upper bound and sample complexity required for any arbitrary \mathbf{q} to converge to \mathbf{q}^* .

Experimentally, we implemented two algorithms, as detailed in Section 3.2: Online-Guidance and Offline-Guidance. We tested their performance in the Gymnasium environment. Results indicate that our framework can prevent invalid exploration and accelerate convergence. Furthermore, it can be applied in complex environments, such as the MuJoCo control tasks.

The main contributions of this paper are:

1. It combines the advantages of both reward shaping techniques and the LLM/VLM Agent framework to improve sample efficiency.
2. It transforms the impact of inaccurate or hallucinatory guidance into the cost of exploration.
3. It supports online correction and can interact with human feedback.
4. Theoretically, this framework can learn from imprecise, incomplete, or cross-domain data sets.

We use Table 1 to display the capabilities of LLM-guided Q-learning compared to other popular frameworks.

	Potential Reward Heuristic	Non-Potential Reward Heuristic	LLM guided Q Heuristic	LLM/VLM agent
Improve sample efficiency	✓	✓	✓	✓
Unbiased Agent Training	✓	-	✓	-
Inaccurate Heuristic Adaptation	-	-	✓	✓
Interactive Training Correction	-	-	✓	✓
Real-Time Inference	✓	✓	✓	-
No Hallucination	✓	✓	✓	-
Complex Task Support	-	✓	✓	-

Table 1: Comparison of Frameworks by Feature

2 Related Work

2.1 Reward Shaping

Reward shaping, initially introduced by [19], is a crucial technique in reinforcement learning (RL) that modifies reward functions to improve agent learning efficiency. This approach has been further refined

to accommodate various learning contexts and challenges. For example, Inverse RL [20, 21, 22] and Preference RL [23, 24, 25, 26], or reward heuristic: unsupervised auxiliary tasks reward [27]; count-based reward heuristics [6, 7]; Self-supervised prediction errors as reward heuristics [28, 29, 30]. As explained in 1, non-potential-based reward shaping introduces biased performance, and potential-based reward shaping can not provide guidance on actions and terminal states. Furthermore, the reward shaping technique suffers from inaccurate guidance.

2.2 LLM/VLM Agent

With limited samples and constraints regulating responses, LLMs/VLMs can achieve few-shot or even zero-shot learning in various contexts, as demonstrated by works such as Voyager [12], ReAct [31], SwiftSage [32], and SuspiciousAgent [33].

In the field of robotics, VIMA [34] employs multimodal learning to enhance agents’ comprehension capabilities. Additionally, the use of LLMs for high-level control is becoming a trend in control tasks [13, 14, 15].

In web search, interactive agents [35, 36, 37] can be constructed using LLMs/VLMs. Moreover, to mitigate the impact of hallucinations, additional frameworks have been developed. For instance, decision reconsideration [38, 39], self-correction [40, 41], and observation summarization [42] have been proposed to address this issue.

2.3 LLM-enhanced RL

Relying on the understanding and generation capabilities of large models, LLM-enhanced RL has become a popular field [17, 43]. Researchers have investigated the diverse roles of large models within reinforcement learning (RL) architectures, including their application in reward design [44, 45, 43, 46, 47, 48], information processing [49, 50, 51], as a policy generator, and as a generator within large language models (LLMs) [52, 53, 54, 55]. While existing work on LLM-assisted reward design reduces design complexity, it either introduces bias into the original Markov Decision Process (MDP) or fails to offer adequate guidance for complex tasks.

3 LLM-guided Q-learning

Figure 1 illustrates the framework of LLM-guided Q-learning. As shown, the LLM provides heuristic values at any iteration step to influence the Q function, which in turn affects the actions of the derived policy in subsequent iterations. It represents a comprehensive training framework aimed at enhancing the sample efficiency of Q-learning algorithms. This approach is marked by its ability to adapt to imprecise heuristics, recovering to its original performance levels after receiving incorrect guidance within a finite number of training steps. Additionally, it supports online corrections and avoids resulting in biased performance, ensuring reliable functionality in dynamic learning environments. This section discusses popular heuristic terms used in Q-learning, highlighting the role of Large Language Models (LLMs) in generating Q-values. Additionally, we introduce two practical implementations designed to effectively deploy this innovative framework.

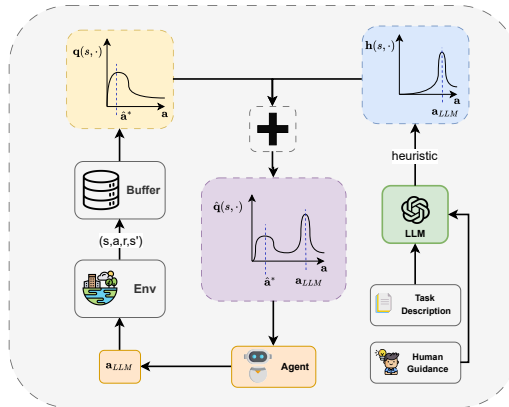


Figure 1: Framework of LLM-guided Q-learning. The update sources for Q-learning include both collected experience and LLM-generated heuristics. The learned \hat{q} values subsequently influence the agent’s behavior in future episodes.

3.1 Heuristic Q-learning Framework

In the Q-learning framework, an experience buffer D is used to store transitions from the Markov Decision Process (MDP), supporting both online and offline training. The Q value is a high-level representation of both the environment and the policy of an agent. It encapsulates key elements such as rewards r , transition probabilities P , states s , actions a , and the policy π , thereby integrating the environmental dynamics and the policy under evaluation. Changes in any of these components directly influence the Q values associated with different actions. Non-potential-based reward designs can bias agent performance, while potential-based designs pose implementation challenges as they do not modify rewards at the action level or in terminal states. Given these challenges, we propose a novel training framework: LLM-guided Q-learning, abandoning traditional reward shaping technique.

The proposed LLM-guided Q-Learning has a general form: $\hat{q} = [\mathbf{q} + \mathbf{h}]$, where $\mathbf{h} : S \times A \rightarrow \mathbb{R}$ is the heuristic term that changes the original Q value. The truncation operator $[\cdot]$ prevents potential Q-function divergence[5] by ensuring input does not exceed $\frac{R_{\max}}{1-\gamma}$. Specifically, the term \mathbf{h} can be of many forms. here we list some popular heuristic term at chart 2.

Expression	Description
$-\log \pi(a s)$ [3]	Negative log-probability of action a given state s , used in the Soft Actor-Critic algorithm.
$\sum_{t=t'}^T \gamma^t r_t$ [9, 56]	Cumulative return of an episode, summed over rewards r_t at each time step t , discounted by factor γ .
$c_{uct} \sqrt{\frac{\log N(s)}{N(s,a)}}$ [57]	UCT heuristic for balancing exploration and exploitation in Monte Carlo Tree Search(MCTS)[57, 58, 59], where c_{uct} is a tunable parameter for exploration emphasis.
$c \sqrt{\frac{H^2 \log(HSA/\delta)}{N_h(s,a) \vee 1}}$ [60]	penalty term in the VI-LCB algorithm for finite-horizon MDPs.
$\mathcal{R}(G(p(s, a)))$ [44] ¹	A generative model outputs the heuristic value directly, based on input prompt p , which includes descriptions of state s , and action a .
$\mathcal{T}(G(p))(s, a)$	A generative model first generates executable code from prompt p that acts as a heuristic function, then evaluates it with inputs s and a .

Table 2: Heuristic Terms and Their Expressions.

Integrating Q-functions with different heuristic functions leads to agents displaying distinct behavioral styles.

Limitations on Maximum Entropy Current popular heuristic Q-learning approaches, such as MCTS and SAC, utilize maximum entropy term or a count bonus term to encourage exploration. These methods are essentially neighbourhood search algorithms. For example, in SAC, denote \hat{a}^* as the optimal action derived from the learned Q-function in state s , and $\hat{a}^* + \epsilon$ is close to \hat{a}^* . We can infer that the value $\hat{q}(s, \hat{a}^* + \epsilon)$ is further increased by the entropy term because $\pi(\hat{a}^* + \epsilon|s) < \pi(\hat{a}^*|s)$. When the exported policy from the current learned Q function deviates significantly from the ground truth optimal policy, the agent wastes a tremendous number of samples exploring areas that stray from the optimal trajectory, leading to sample inefficiency. This limitation also explains why the same algorithm performs differently even in the same environment. This challenge has inspired us to develop more advanced heuristics that accelerate training process.

Recent studies[18, 44, 61, 47, 48] in LLM-enhanced reinforcement learning (RL) have used LLMs to generate rewards or reward functions, which can bias agent performance or slow down training due to the time required for generating reward signals on a step-by-step basis. By using LLMs to generate heuristic Q-values instead, we overcome issues associated with reward shaping. This approach enables action-level heuristic values and avoids biasing agent capabilities after convergence.

¹This paper allows the LLM to generate rewards; however, the formula can also serve as a Q-value heuristic.

3.2 Algorithm Implementation

In the implementation of LLM-guided Q-learning, We provide two kinds of algorithm: offline guidance Q learning and online guidance Q learning. The offline guidance Q learning is a special case of online guidance Q learning which only provides guidance at iteration step $k = 0$. We adapted the loss function from the traditional TD3 algorithm[4] to accommodate the error associated with the generated heuristic Q-values. We employ an L2 loss to approximate the data sampled from the Markov Decision Process (MDP), defined as:

$$L_{major}(\theta) = E_{(s,a,r,s') \sim D} [([r + \gamma \min_i \hat{\mathbf{q}}_{\theta_i}(s', \hat{a} + \epsilon)] - \hat{Q}_{\theta}(s, a))^2] \quad (1)$$

We apply the truncation operator $\lceil \cdot \rceil$ to the target Q value to prevent potential divergence examples while ensuring that it is consistent with our theoretical analysis assumptions.

The pseudo-code of offline guidance Q learning is displayed at algorithm 1. In algorithm 1, two additional step is added to the TD3 algorithm: Q-buffer Generation and Q bootstrapping. For Q-buffer Generation, the input p is the combination of task description, and predefined prompt. Task description contains specific descriptions of state-actions and provides conditions for trajectory termination. Treating text descriptions as input to the large model can help it better generate Q values. In order to constrain the model’s answers, we developed a general template, which can be combined with the description of any task to form the input of the large model. Its main task is to guide the LLM to generate an executable python function, which will return two set of (s, a, Q) pairs.

To facilitate Q bootstrapping, the tuples returned from previous step constitute the Q buffer D_g , defined as :

$$D_g := \{(s_i, a_i, Q_i) \mid (s_i, a_i, Q_i) \in D(G(p)), i = 1, 2, \dots, n\}$$

Note that we use $D(\cdot)$ to denote the transformation of LLM-generated text into a set of (s, a, Q) pairs. Subsequently, we employ the following loss function to bootstrap the estimated \hat{Q} :

$$L_{bootstrap}(\theta) = E_{(s_i, a_i, Q_i) \sim D_g} (Q_i - \hat{\mathbf{q}}_{\theta}(s_i, a_i))^2 \quad (2)$$

Algorithm 1 Offline Guidance Q Learning Algorithm

- 1: **Inputs:** Local MDP D , Large Language Model G , prompt p ,
 - 2: **Initialization:** Initialize Heuristic: $G(p)$, initialize actor-critic $(\mu_{\phi}, Q_{\theta_1}, Q_{\theta_2})$ and target actor-critic $(\mu_{\phi'}, Q_{\theta'_1}, Q_{\theta'_2})$
 - 3: **Generate Q buffer:** $D_g \leftarrow \{(s_i, a_i, Q_i) \mid (s_i, a_i, Q_i) = G(p), i = 1, 2, \dots, n\}$
 - 4: **Q Bootstrapping:** $\theta = \theta - \alpha \nabla_{\theta} L_{bootstrap}$ using eq 2
 - 5: **for** iteration $t' \in T = 1, 2, 3 \dots$ **do**
 - 6: Sample (s, a, r, s') from Env
 - 7: $D \leftarrow D \cup (s, a, r, s')$
 - 8: Sample N transitions (s, a, r, s') from D
 - 9: $\hat{a} \leftarrow \mu(s') + \epsilon, \epsilon \sim \text{clip}(\mathcal{N}(0, \sigma), -c, c)$
 - 10: $y(s') \leftarrow \lceil r + \gamma \min_{i=1,2} \mathbf{q}_{\theta_i}(s', \hat{a}) \rceil$
 - 11: Update critics $\theta_i \leftarrow \arg \min_{\theta_i} L_{major}(\theta_i)$
 - 12: **if** $t' \bmod d$ **then**
 - 13: Update actor $\phi \leftarrow \arg \min_{\phi} L_{actor}(\phi)$
 - 14: Update target networks:
 - 15: $\theta'_i \leftarrow \tau \theta_i + (1 - \tau) \theta'_i$
 - 16: $\phi' \leftarrow \tau \phi + (1 - \tau) \phi'$
 - 17: **end if**
 - 18: **end for**
 - 19: **end while**
-

GPT4’s ability to predict Q-values will decrease as the complexity of the environment increases, and Offline Guidance cannot predict in advance all potential problems encountered by the agent during the training process, therefore, we propose Online Guidance, a method that enables the agent to receive guidance at any training step from various sources. The corresponding expression for online heuristic Q-learning is presented in Equation 3:

$$L_{online}(\theta) = L_{major}(\theta) + E_{(s_i, a_i, Q_i) \sim D(G(p))} [(\hat{\mathbf{q}}_{\theta}(s_i, a_i) - Q_i)^2] \quad (3)$$

With equation 3, we now display the pseudo-code of Online Guidance Q learning Algorithm at Appendix C.

The Online Guidance algorithm detects whether there is guidance from external sources at each training step. In our experiments, we utilize human feedback as the heuristic Q function. If the agent engages in ineffective exploration, humans will offer guidance information, which the language model then transforms into (s, a, Q) pairs. A visualization for online guidance can be viewed at Figure 2.

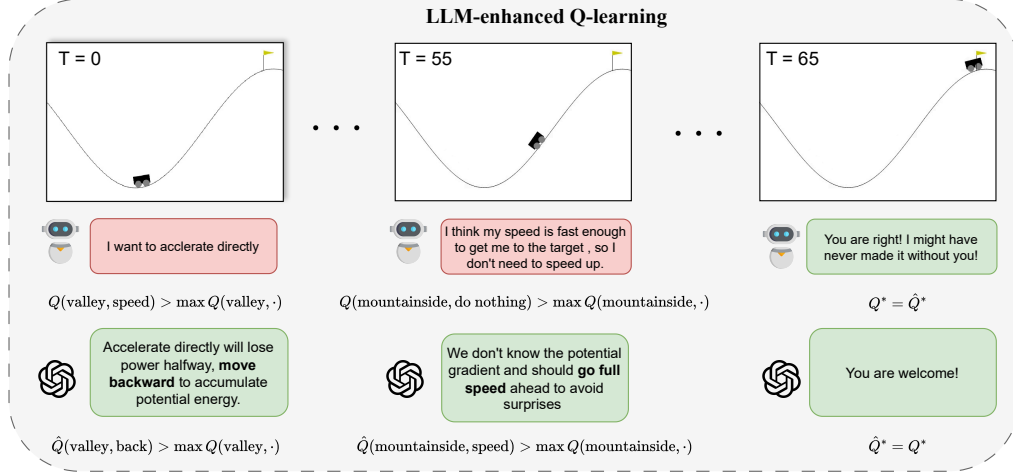


Figure 2: Overview of the Online Guidance Q-learning framework. External guidance can be provided at any training step, offering heuristic Q-values that influence policy decisions and improve sample efficiency.

4 Theoretical Analysis

4.1 Suboptimality Analysis

Define $a^* = \arg \max_a \mathbf{q}^*(s, a)$. Similarly, define $a^{\pi_D} = \arg \max_a \mathbf{q}_D^*(s, a)$, a^π denotes $\max_a \pi(a|s)$ of any random policy π . Then we have:

$$\mathbf{q}^*(s, a^*) - (\mathbf{q}^{\pi_D})^*(s, a^{\pi_D}) \leq \underbrace{\inf_{\pi} \left(\mathbf{q}^*(s, a^{\pi^*}) - \hat{\mathbf{q}}_D^*(s, a^{\pi^*}) \right)}_{(A)} + \underbrace{\left(\hat{\mathbf{q}}_D^*(s, a^{\pi^*}) - (\hat{\mathbf{q}}_D^\pi)^*(s, a^\pi) \right)}_{(B)} + \sup_{\pi} \left((\hat{\mathbf{q}}_D^\pi)^*(s, a^\pi) - (\mathbf{q}^\pi)^*(s, a^\pi) \right)$$

Proof. see proof at B.2 □

The first segment, Item (A), evaluates the divergence between the Q-function derived from the sampled MDP D and the optimal Q-function. For any state s , subterm (A1) represents overestimation by using the optimal action a^* to measure the difference between the Q-value of the optimal action in D and the Q-value of the actual optimal action. Sub-item (A2) analyzes the difference in Q values of different policies. Item (A) assesses whether the buffer MDP D effectively captures optimal trajectories. If so, minimizing Item A is viable as it confirms that the optimal action in the buffer MDP aligns with the true optimal action. Item (B) measures the difference in Q values of different policies. If D does not contain the optimal trajectory, the gap will persist throughout training. The introduction of a heuristic term aims to bridge this gap and guide the policy toward sampling the

optimal trajectory. Subsequently, we will provide the upper bound of the function and the sample complexity required for $\hat{\mathbf{q}}_D$ to converge to the optimal \mathbf{q}^* .

4.2 Impact of Hallucination

The hallucination problem in large language models (LLMs) manifests in two primary ways: the generation of verbose responses that fail to meet specified requirements and the production of inaccurate Q-values. These imprecise Q-values can be further categorized into overestimation and underestimation.

Overestimation has been clearly discussed in TD3[4]. The main point of overestimation is that the error ϵ on the target will influence the TD update and thus impact all the Q values of previous state-action pairs.

The impact of underestimation bias can be divided into two situations: the underestimation of non-optimal actions and the underestimation of optimal actions. We define $a^* := \arg \max_a \mathbf{q}^*(s, a)$, and $\hat{a}^* = \arg \max_a \hat{\mathbf{q}}(s, a)$.

Underestimation on Non-Optimal Actions Assume that for some non-optimal action a , $\hat{\mathbf{q}}(s, a) < \mathbf{q}^*(s, a) \leq \mathbf{q}^*(s, a^*)$. This means that the learned Q function underestimates non-optimal action a . According to the definition of the greedy sampling policy μ , this underestimation setting will not impact the policy, and only \hat{a}^* will.

Underestimation on Optimal Actions We can separate underestimation on optimal actions into two cases. Case 1: $\hat{a}^* = a^*$, and Case 2 : $\hat{a}^* \neq a^*$. Both cases satisfies: $\hat{\mathbf{q}}(s, \hat{a}^*) < \mathbf{q}^*(s, a^*)$

Case 1: The derived policy will not be influenced by the underestimation, because the Q function and the policy function have a bijective relations. In Case 1, the relationship between \mathbf{q}^* and $\hat{\mathbf{q}}$ can be expressed as $\mathbf{q}^*(s, a^*) > \hat{\mathbf{q}}(s, a^*) > \text{secmax}_a \hat{\mathbf{q}}(s, a)$ and the exported policy is the same , which won't influence the performance of the agent. This explains why CQL [62] is still successful even with pessimistic Q-values.

Case 2: With the assumption $\hat{a}^* \neq a^*$, we can derive that $:\hat{\mathbf{q}}(s, a^*) < \max_a \hat{\mathbf{q}}(s, a) < \mathbf{q}^*(s, a^*)$. This kind of underestimation will impact the performance of the agent since the optimal action of the learned Q function isn't the ground truth optimal action. To solve this problem, we either improve the value of a^* or decrease the value of other non-optimal actions. However, decreasing the value of all other non-optimal actions is impossible ,as it's computationally complex. Another feasible method to make a^* optimal in the learned Q function is to improve by sampling a high discounted return trajectory that includes a^* , or use a heuristic term to force a^* to be optimal in $\hat{\mathbf{q}}(s, \cdot)$.

The analysis results tell us that underestimation of non-optimal action will not impact the agent's performance and can help avoid ineffective exploration. There is no strict limitation on the Q-value estimation of the optimal action, thus inaccurate guidance will not impact the performance of the agent according to Case 1. When D includes the optimal trajectory , $\hat{\mathbf{q}}$ will converge to \mathbf{q}^* very soon. We then proof that $\hat{\mathbf{q}}^* = \mathbf{q}^*$ and provide the upper bound of $|\mathbf{q}_D - \mathbf{q}^*|$ and the sample complexity for \mathbf{q} converging to \mathbf{q}^*

4.3 Convergence Analysis

Theorem 1. $\hat{\mathbf{q}}$ is a contraction defined in metrics space (\mathcal{X}, l_∞) , i.e:

$$\|\mathcal{B}_D(\hat{\mathbf{q}}) - \mathcal{B}_D(\hat{\mathbf{q}}')\|_\infty \leq \gamma \|\hat{\mathbf{q}} - \hat{\mathbf{q}}'\|_\infty$$

Since both $\hat{\mathbf{q}}$ and \mathbf{q} are updated on the same MDP, we have the following equation:

$$\hat{\mathbf{q}}_D^* = \mathbf{q}_D^*$$

Proof. See Appendix B.1 □

Assume that LLM provides a relatively high heuristic Q value for state-action pair $\langle s', a' \rangle$ at training step k. and it satisfies $:\max_\tau G_k(\tau) < \mathbf{q}^k(s', a') + \mathbf{h}^k(s', a')$. This inequality can also be expressed

as:

$$\max_{s,a} \mathbf{q}(s, a) < \mathbf{q}^k(s', a') + \mathbf{h}^k(s', a')$$

As the $\hat{\mathbf{q}}$ is updated using next state’s Q value, then we have the following inequality:

$$\hat{\mathbf{q}}^k(s', a') > \max_{s,a} \mathbf{q}^k(s, a) \geq \max_a \mathbf{q}^k(s', a)$$

This makes a' the optimal action in $\hat{\mathbf{q}}(s', a')$ at training step k . In online training process, $\mu(s')$ will directly execute a' in the next following training step, allowing the agent to avoid exploring non-optimal trajectories. Moreover, $\hat{\mathbf{q}}$ will gradually converge towards the fixed point of MDP D as the training step increases, according to Theorem 1.

Compared to reward shaping techniques, our framework avoids introducing biases into the agent’s performance and facilitates rapid learning with LLMs. Next, we establish the upper bound of \mathbf{q}_D and determine the sample complexity required for \mathbf{q}_D to converge to \mathbf{q}^* .

Theorem 2 (Convergence Bound). *Suppose that s' and r are sampled iid from $P(\cdot|s, a)$ and $R(\cdot|s, a)$, then with probability at least $1 - \delta$:*

$$|\mathbf{q}_D^*(s, \mu(s)) - \mathbf{q}^*(s, \mu(s))| \leq \left(\sqrt{\frac{1}{2} \ln \frac{2|S \times A|}{\delta}} \right) \sum_{s'} \nu_D(s'|s_0 = s) \frac{1}{\sqrt{\mathfrak{n}_D(\langle s', \mu(s') \rangle)}}$$

Proof. see proof at B.3 □

In this bound, we denote $\nu_D(s'|s_0 = s)$ as $\frac{1}{1-\gamma} (\mathbf{I} - \gamma \mathbf{P}_D)^{-1}(s, s')$, representing the discounted visitation probability of state s' starting from s . The bound is influenced by $\mathfrak{n}_D(\langle s', \mu(s') \rangle)$; specifically, the greater the amount of sampled data at $(s, \mu(s))$, the lower the bound will be.

Theorem 3 (Convergence Sample Complexity). *The sample complexity n required for \mathbf{q} to converge to the optimal fixed-point \mathbf{q}^* with probability $1 - \delta$ is:*

$$n > \mathcal{O} \left(\frac{|S|^2}{2\epsilon^2} \ln \frac{2|S \times A|}{\delta} \right)$$

Proof. see proof at B.4. □

Theorem 3 indicates that the sample complexity depends on the size of the state and action spaces. Additionally, it asserts that the hallucination guidance provided by large language models (LLMs) will be eliminated within a finite number of steps.

5 Experiment

We evaluate our proposed algorithm across eight Gymnasium environments, ranging from the simplest MountainCar to the more complex Humanoid Run. Our objective is to determine whether LLM-guided Q-learning accelerates training process. In this experiment, the LLM heuristic term is integrated with TD3 [4], forming $TD3^*$. Specifically, we compare $TD3^*$ with four widely used baselines and assess convergence speed to determine each algorithm’s sample efficiency.

Environment setting We choose 3 simple tasks from classical control : *cartpole, mountaincarcontinuous, pendulum*, and 5 complex tasks from Mujoco: *ant, halfcheetah, hopper, humanoid, walker2d*.²

²Please see gymnasium.farama.org for more details.

Evaluation we evaluate each algorithm’s sample efficiency through convergence speed. When the agent’s performance stop fluctuating greatly, the agent is considered converged. Since the agent’s performance may impact by the randomness of environment and initialization, each algorithm will run 10 times in each task, and the average score of 10 runs will be used as evaluation result. In the training process, value iteration and performance evaluation process alternately, there is a sample limit, normally set to $1e6$, every time the agent samples $1e3$ steps, we conduct an algorithm performance verification. The process of performance verification is: it will use the current strategy to interact with the environment ten times, and then finally take the average as the performance verification of the algorithm.

Baseline In terms of baseline selection, we compare our model with several of the most popular algorithms, namely: PPO, SAC, TD3, and DDPG. Our approach, termed LLM-guided Q learning, extends the TD3 framework and is referred to as $TD3^*$. In Table 3, the "Guidance Count" represents the number of (s, a, Q) pairs provided by the LLM after analyzing the task description. In our algorithm implementation, we categorize these pairs into two types: good Q pairs and bad Q pairs. Good Q pairs are those that the LLM deems conducive to hastening the agent’s convergence, whereas bad Q pairs are considered by the LLM to prevent ineffective exploration by the agent.

Guidance Count			Env	Algorithms				
good Q	bad Q	ISI+AI		PPO	SAC	DDPG	TD3	$TD3^*$
2	2	2+1	mountainCarContinuous	Failed	Failed	Failed	Failed	140k
0	0	3+1	pendulum				28k	
0	0	4+1	cartpole					
0	2	11+3	hopper				600k	400k
0	2	17+6	walker2d				372k	262k
0	0	17+6	halfcheetah					
0	1	27+8	ant				400k	399k
0	2	376+17	humanoid				550k	465k

Table 3: Comparative Analysis of Convergence Speed and Guidance Impact on LLM-guided Q-learning Across Environments

Implementation In our algorithm implementation, we employ GPT-4 as the LLM. In Table 3, $TD3^*$ utilizes offline guidance, where the LLM generates (s, a, Q) pairs directly and in a one-time fashion based on human prompts and task descriptions. Prior to the agent beginning sampling, the Q function is trained directly to fit the heuristic values provided by the LLM. In selecting some key parameters for TD3, we set the *policy_exploration* to 0.2 and *target_noise* to 0.2. The purpose of these settings is to enhance the local exploration capabilities of the TD3 algorithm and to smooth the Q values to prevent overfitting.

5.1 TD Error Distribution in Terminal and Non-Terminal States

The loss curve of the Q-function is a crucial indicator of an agent’s performance. A high loss implies that the Q-function does not accurately represent the collected MDP, potentially resulting in poor agent performance.

Evaluation In this section, we use the Hopper environment as an illustrative example and present two figures: the value distribution of non-terminal states and the value distribution of terminal states.

Result Analysis From the results shown in Figure X, we observe that the values of terminal states are generally distributed above 1000, while those of non-terminal states are predominantly below 100. This finding underscores that an agent’s performance can change significantly when encountering a new terminal state.

Performance Fluctuations When agent reach peak performance, the agent’s performance will drop sometimes and then recover in a few episodes. This phenomenon is caused by the chain reaction of TD updates. The TD updates can be considered as supervised learning of linked list data. When TD error forces Q function to fit new terminal states(as displayed at figure X , all related previous $\langle s, a \rangle$ pairs’ Q value will be influenced and thus cause performance drop.

6 Discussion and Limitation

This work integrates the advantages of generative models and reinforcement learning, addressing the limitations of both approaches. Its primary contribution is enabling agents to learn from imprecise data. By utilizing TD error-based Q-value iteration, the method transforms the cost induced by hallucination into a cost of exploration. Specifically, it shifts the burden of creating precise, high-quality, target-aligned datasets to the cost of exploration, thus facilitating development in areas like imitation learning and generative reinforcement learning on imperfect datasets. Moreover, when extensive exploration is allowed, agents can discover superior trajectories based on guidance trajectories, thereby achieving or even surpassing expert performance in many tasks more quickly.

Furthermore, our training framework supports the development of autonomous agents, such as autonomous soccer robots [63, 64]. A sparse reward function can be implemented for these robots, offering rewards for goals and penalties for fouls. The provided guidance is then translated into heuristic Q-values through generative models to improve Q-learning. Ultimately, the robots can identify the most effective goal-scoring strategies through limited interactions.

However, there is significant room for improvement. We have not tested the framework in visual environments, and due to the limitations of large language models’ comprehension abilities, its performance on complex humanoid robots is suboptimal, as it fails to provide action-level guidance.

References

- [1] Christopher JCH Watkins and Peter Dayan. Q-learning. *Machine learning*, 8:279–292, 1992.
- [2] Timothy P Lillicrap, Jonathan J Hunt, Alexander Pritzel, Nicolas Heess, Tom Erez, Yuval Tassa, David Silver, and Daan Wierstra. Continuous control with deep reinforcement learning. *arXiv preprint arXiv:1509.02971*, 2015.
- [3] Tuomas Haarnoja, Aurick Zhou, Kristian Hartikainen, George Tucker, Sehoon Ha, Jie Tan, Vikash Kumar, Henry Zhu, Abhishek Gupta, Pieter Abbeel, et al. Soft actor-critic algorithms and applications. *arXiv preprint arXiv:1812.05905*, 2018.
- [4] Scott Fujimoto, Herke Hoof, and David Meger. Addressing function approximation error in actor-critic methods. In *International conference on machine learning*, pages 1587–1596. PMLR, 2018.
- [5] Zaiwei Chen, John-Paul Clarke, and Siva Theja Maguluri. Target network and truncation overcome the deadly triad in-learning. *SIAM Journal on Mathematics of Data Science*, 5(4):1078–1101, 2023.
- [6] Marc Bellemare, Sriram Srinivasan, Georg Ostrovski, Tom Schaul, David Saxton, and Remi Munos. Unifying count-based exploration and intrinsic motivation. *Advances in neural information processing systems*, 29, 2016.
- [7] Georg Ostrovski, Marc G Bellemare, Aäron Oord, and Rémi Munos. Count-based exploration with neural density models. In *International conference on machine learning*, pages 2721–2730. PMLR, 2017.
- [8] Haoran Tang, Rein Houthooft, Davis Foote, Adam Stooke, OpenAI Xi Chen, Yan Duan, John Schulman, Filip DeTurck, and Pieter Abbeel. # exploration: A study of count-based exploration for deep reinforcement learning. *Advances in neural information processing systems*, 30, 2017.
- [9] Sinong Geng, Aldo Pacchiano, Andrey Kolobov, and Ching-An Cheng. Improving offline rl by blending heuristics. *arXiv preprint arXiv:2306.00321*, 2023.
- [10] Ching-An Cheng, Andrey Kolobov, and Adith Swaminathan. Heuristic-guided reinforcement learning. *Advances in Neural Information Processing Systems*, 34:13550–13563, 2021.
- [11] Ethan Brooks, Logan Walls, Richard L Lewis, and Satinder Singh. Large language models can implement policy iteration. *Advances in Neural Information Processing Systems*, 36, 2024.
- [12] Guanzhi Wang, Yuqi Xie, Yunfan Jiang, Ajay Mandlekar, Chaowei Xiao, Yuke Zhu, Linxi Fan, and Anima Anandkumar. Voyager: An open-ended embodied agent with large language models. *arXiv preprint arXiv:2305.16291*, 2023.

- [13] Lucy Xiaoyang Shi, Zheyuan Hu, Tony Z Zhao, Archit Sharma, Karl Pertsch, Jianlan Luo, Sergey Levine, and Chelsea Finn. Yell at your robot: Improving on-the-fly from language corrections. *arXiv preprint arXiv:2403.12910*, 2024.
- [14] Huihan Liu, Alice Chen, Yuke Zhu, Adith Swaminathan, Andrey Kolobov, and Ching-An Cheng. Interactive robot learning from verbal correction. *arXiv preprint arXiv:2310.17555*, 2023.
- [15] Yutao Ouyang, Jinhan Li, Yunfei Li, Zhongyu Li, Chao Yu, Koushil Sreenath, and Yi Wu. Long-horizon locomotion and manipulation on a quadrupedal robot with large language models. *arXiv preprint arXiv:2404.05291*, 2024.
- [16] Zirui Zhao, Wee Sun Lee, and David Hsu. Large language models as commonsense knowledge for large-scale task planning. *Advances in Neural Information Processing Systems*, 36, 2024.
- [17] Yuqing Du, Olivia Watkins, Zihan Wang, Cédric Colas, Trevor Darrell, Pieter Abbeel, Abhishek Gupta, and Jacob Andreas. Guiding pretraining in reinforcement learning with large language models. In *International Conference on Machine Learning*, pages 8657–8677. PMLR, 2023.
- [18] Yufei Wang, Zhanyi Sun, Jesse Zhang, Zhou Xian, Erdem Biyik, David Held, and Zackory Erickson. RL-vlm-f: Reinforcement learning from vision language foundation model feedback. *arXiv preprint arXiv:2402.03681*, 2024.
- [19] Andrew Y Ng, Daishi Harada, and Stuart Russell. Policy invariance under reward transformations: Theory and application to reward shaping. In *Icml*, volume 99, pages 278–287, 1999.
- [20] Brian D Ziebart, Andrew L Maas, J Andrew Bagnell, Anind K Dey, et al. Maximum entropy inverse reinforcement learning. In *Aaai*, volume 8, pages 1433–1438. Chicago, IL, USA, 2008.
- [21] Markus Wulfmeier, Peter Ondruska, and Ingmar Posner. Maximum entropy deep inverse reinforcement learning. *arXiv preprint arXiv:1507.04888*, 2015.
- [22] Chelsea Finn, Sergey Levine, and Pieter Abbeel. Guided cost learning: Deep inverse optimal control via policy optimization. In *International conference on machine learning*, pages 49–58. PMLR, 2016.
- [23] Paul F Christiano, Jan Leike, Tom Brown, Miljan Martic, Shane Legg, and Dario Amodei. Deep reinforcement learning from human preferences. *Advances in neural information processing systems*, 30, 2017.
- [24] Borja Ibarz, Jan Leike, Tobias Pohlen, Geoffrey Irving, Shane Legg, and Dario Amodei. Reward learning from human preferences and demonstrations in atari. *Advances in neural information processing systems*, 31, 2018.
- [25] Kimin Lee, Laura Smith, and Pieter Abbeel. Pebble: Feedback-efficient interactive reinforcement learning via relabeling experience and unsupervised pre-training. *arXiv preprint arXiv:2106.05091*, 2021.
- [26] Jongjin Park, Younggyo Seo, Jinwoo Shin, Honglak Lee, Pieter Abbeel, and Kimin Lee. Surf: Semi-supervised reward learning with data augmentation for feedback-efficient preference-based reinforcement learning. In *10th International Conference on Learning Representations, ICLR 2022*. International Conference on Learning Representations, 2022.
- [27] Max Jaderberg, Volodymyr Mnih, Wojciech Marian Czarnecki, Tom Schaul, Joel Z Leibo, David Silver, and Koray Kavukcuoglu. Reinforcement learning with unsupervised auxiliary tasks. In *International Conference on Learning Representations*, 2016.
- [28] Deepak Pathak, Pulkit Agrawal, Alexei A Efros, and Trevor Darrell. Curiosity-driven exploration by self-supervised prediction. In *International conference on machine learning*, pages 2778–2787. PMLR, 2017.
- [29] Bradley C Stadie, Sergey Levine, and Pieter Abbeel. Incentivizing exploration in reinforcement learning with deep predictive models. *arXiv preprint arXiv:1507.00814*, 2015.
- [30] Pierre-Yves Oudeyer and Frederic Kaplan. What is intrinsic motivation? a typology of computational approaches. *Frontiers in neurorobotics*, 1:108, 2007.
- [31] Shunyu Yao, Jeffrey Zhao, Dian Yu, Nan Du, Izhak Shafran, Karthik Narasimhan, and Yuan Cao. React: Synergizing reasoning and acting in language models. *arXiv preprint arXiv:2210.03629*, 2022.

- [32] Bill Yuchen Lin, Yicheng Fu, Karina Yang, Faeze Brahman, Shiyu Huang, Chandra Bhagavatula, Prithviraj Ammanabrolu, Yejin Choi, and Xiang Ren. Swiftsage: A generative agent with fast and slow thinking for complex interactive tasks. *Advances in Neural Information Processing Systems*, 36, 2024.
- [33] Jiaxian Guo, Bo Yang, Paul Yoo, Bill Yuchen Lin, Yusuke Iwasawa, and Yutaka Matsuo. Suspicion-agent: Playing imperfect information games with theory of mind aware gpt-4. *arXiv preprint arXiv:2309.17277*, 2023.
- [34] Yunfan Jiang, Agrim Gupta, Zichen Zhang, Guanzhi Wang, Yongqiang Dou, Yanjun Chen, Li Fei-Fei, Anima Anandkumar, Yuke Zhu, and Linxi Fan. Vima: General robot manipulation with multimodal prompts. In *NeurIPS 2022 Foundation Models for Decision Making Workshop*, 2022.
- [35] Izzeddin Gur, Hiroki Furuta, Austin Huang, Mustafa Safdari, Yutaka Matsuo, Douglas Eck, and Aleksandra Faust. A real-world webagent with planning, long context understanding, and program synthesis. *arXiv preprint arXiv:2307.12856*, 2023.
- [36] Peter Shaw, Mandar Joshi, James Cohan, Jonathan Berant, Panupong Pasupat, Hexiang Hu, Urvashi Khandelwal, Kenton Lee, and Kristina N Toutanova. From pixels to ui actions: Learning to follow instructions via graphical user interfaces. *Advances in Neural Information Processing Systems*, 36, 2024.
- [37] Shuyan Zhou, Frank F Xu, Hao Zhu, Xuhui Zhou, Robert Lo, Abishek Sridhar, Xianyi Cheng, Yonatan Bisk, Daniel Fried, Uri Alon, et al. Webarena: A realistic web environment for building autonomous agents. *arXiv preprint arXiv:2307.13854*, 2023.
- [38] Shunyu Yao, Dian Yu, Jeffrey Zhao, Izhak Shafran, Tom Griffiths, Yuan Cao, and Karthik Narasimhan. Tree of thoughts: Deliberate problem solving with large language models. *Advances in Neural Information Processing Systems*, 36, 2024.
- [39] Jieyi Long. Large language model guided tree-of-thought. *arXiv preprint arXiv:2305.08291*, 2023.
- [40] Noah Shinn, Beck Labash, and Ashwin Gopinath. Reflexion: an autonomous agent with dynamic memory and self-reflection. *arXiv preprint arXiv:2303.11366*, 2023.
- [41] Geunwoo Kim, Pierre Baldi, and Stephen McAleer. Language models can solve computer tasks. *Advances in Neural Information Processing Systems*, 36, 2024.
- [42] Abishek Sridhar, Robert Lo, Frank F Xu, Hao Zhu, and Shuyan Zhou. Hierarchical prompting assists large language model on web navigation. In *The 2023 Conference on Empirical Methods in Natural Language Processing*, 2023.
- [43] Thomas Carta, Clément Romac, Thomas Wolf, Sylvain Lamprier, Olivier Sigaud, and Pierre-Yves Oudeyer. Grounding large language models in interactive environments with online reinforcement learning. In *International Conference on Machine Learning*, pages 3676–3713. PMLR, 2023.
- [44] Minae Kwon, Sang Michael Xie, Kalesha Bullard, and Dorsa Sadigh. Reward design with language models. *arXiv preprint arXiv:2303.00001*, 2023.
- [45] Yue Wu, Yewen Fan, Paul Pu Liang, Amos Azaria, Yuanzhi Li, and Tom M Mitchell. Read and reap the rewards: Learning to play atari with the help of instruction manuals. *Advances in Neural Information Processing Systems*, 36, 2024.
- [46] Kun Chu, Xufeng Zhao, Cornelius Weber, Mengdi Li, and Stefan Wermter. Accelerating reinforcement learning of robotic manipulations via feedback from large language models. *arXiv preprint arXiv:2311.02379*, 2023.
- [47] Wenhao Yu, Nimrod Gileadi, Chuyuan Fu, Sean Kirmani, Kuang-Huei Lee, Montserrat Gonzalez Arenas, Hao-Tien Lewis Chiang, Tom Erez, Leonard Hasenclever, Jan Humplik, et al. Language to rewards for robotic skill synthesis. In *7th Annual Conference on Robot Learning*, 2023.
- [48] Yecheng Jason Ma, William Liang, Guanzhi Wang, De-An Huang, Osbert Bastani, Dinesh Jayaraman, Yuke Zhu, Linxi Fan, and Anima Anandkumar. Eureka: Human-level reward design via coding large language models. In *The Twelfth International Conference on Learning Representations*, 2023.

- [49] Fabian Paischer, Thomas Adler, Vihang Patil, Angela Bitto-Nemling, Markus Holzleitner, Sebastian Lehner, Hamid Eghbal-Zadeh, and Sepp Hochreiter. History compression via language models in reinforcement learning. In *International Conference on Machine Learning*, pages 17156–17185. PMLR, 2022.
- [50] Fabian Paischer, Thomas Adler, Markus Hofmarcher, and Sepp Hochreiter. Semantic helm: A human-readable memory for reinforcement learning. *Advances in Neural Information Processing Systems*, 36, 2024.
- [51] Alec Radford, Jong Wook Kim, Chris Hallacy, Aditya Ramesh, Gabriel Goh, Sandhini Agarwal, Girish Sastry, Amanda Askell, Pamela Mishkin, Jack Clark, et al. Learning transferable visual models from natural language supervision. In *International conference on machine learning*, pages 8748–8763. PMLR, 2021.
- [52] Lili Chen, Kevin Lu, Aravind Rajeswaran, Kimin Lee, Aditya Grover, Misha Laskin, Pieter Abbeel, Aravind Srinivas, and Igor Mordatch. Decision transformer: Reinforcement learning via sequence modeling. *Advances in neural information processing systems*, 34:15084–15097, 2021.
- [53] Vincent Micheli, Eloi Alonso, and François Fleuret. Transformers are sample-efficient world models. *arXiv preprint arXiv:2209.00588*, 2022.
- [54] Jan Robine, Marc Höftmann, Tobias Uelwer, and Stefan Harmeling. Transformer-based world models are happy with 100k interactions. *arXiv preprint arXiv:2303.07109*, 2023.
- [55] Chang Chen, Yi-Fu Wu, Jaesik Yoon, and Sungjin Ahn. Transdreamer: Reinforcement learning with transformer world models. *arXiv preprint arXiv:2202.09481*, 2022.
- [56] Zichuan Lin, Tianqi Zhao, Guangwen Yang, and Lintao Zhang. Episodic memory deep q-networks. In *Proceedings of the 27th International Joint Conference on Artificial Intelligence*, pages 2433–2439, 2018.
- [57] Levente Kocsis and Csaba Szepesvári. Bandit based monte-carlo planning. In *European conference on machine learning*, pages 282–293. Springer, 2006.
- [58] Cameron B Browne, Edward Powley, Daniel Whitehouse, Simon M Lucas, Peter I Cowling, Philipp Rohlfshagen, Stephen Tavener, Diego Perez, Spyridon Samothrakis, and Simon Colton. A survey of monte carlo tree search methods. *IEEE Transactions on Computational Intelligence and AI in games*, 4(1):1–43, 2012.
- [59] Rémi Coulom. Efficient selectivity and backup operators in monte-carlo tree search. In *International conference on computers and games*, pages 72–83. Springer, 2006.
- [60] Paria Rashidinejad, Banghua Zhu, Cong Ma, Jiantao Jiao, and Stuart Russell. Bridging offline reinforcement learning and imitation learning: A tale of pessimism. *Advances in Neural Information Processing Systems*, 34:11702–11716, 2021.
- [61] Hengyuan Hu and Dorsa Sadigh. Language instructed reinforcement learning for human-ai coordination. In *International Conference on Machine Learning*, pages 13584–13598. PMLR, 2023.
- [62] Aviral Kumar, Aurick Zhou, George Tucker, and Sergey Levine. Conservative q-learning for offline reinforcement learning. *Advances in Neural Information Processing Systems*, 33:1179–1191, 2020.
- [63] Miguel Abreu, Luis Paulo Reis, and Nuno Lau. Designing a skilled soccer team for robocup: Exploring skill-set-primitives through reinforcement learning. *arXiv preprint arXiv:2312.14360*, 2023.
- [64] Tuomas Haarnoja, Ben Moran, Guy Lever, Sandy H Huang, Dhruva Tirumala, Jan Humplik, Markus Wulfmeier, Saran Tunyasuvunakool, Noah Y Siegel, Roland Hafner, et al. Learning agile soccer skills for a bipedal robot with deep reinforcement learning. *arXiv preprint arXiv:2304.13653*, 2023.

A Problem Statement

A.1 Notation

Vectors are denoted by bold lowercase letters, \mathbf{a} , and matrices by uppercase letters, A . Individual vector elements or matrix rows are referenced using function notation, $\mathbf{a}(x)$. The identity matrix is represented as I . We use the notation $\mathbb{E}_p[\cdot]$ to denote the average value of a function under a distribution p , i.e. for any space \mathcal{X} , distribution $p \in \text{dist}(\mathcal{X})$, and function $\mathbf{a} : \mathcal{X} \rightarrow \mathbb{R}$, we have $\mathbb{E}_p[\mathbf{a}] := \mathbb{E}_{x \sim p}[\mathbf{a}(x)]$. For vectors and matrices, we use $\langle, \rangle, \leq, \geq$ to indicate element-wise comparisons. The notation $|\cdot|$ denotes the element-wise absolute value of a vector, with $|\mathbf{a}|(x) = |\mathbf{a}(x)|$. The infinity norm, $|\mathbf{a}|_\infty$, represents the maximum absolute value among the elements of \mathbf{a} .

We define $G : \mathbb{R}^n \rightarrow \mathbb{R}^n$ as the LLM Generator, where n denotes the context length. The prompt p_0 serves as a guiding template to direct the LLM’s output towards generating Python code. In our implementation, the input to G is the concatenation of p_0 and the task description, resulting in an executable Python method that outputs tuples (s, a, Q) . To represent the transformation from text to function or dataset. We denote $\mathcal{T}(\cdot)$ as the transformation from text to function, and use $\mathcal{R}(\cdot)$ to denote the transformation from text to reward.

Markov Decision Processes. We represent the environment with which we are interacting as a Markov Decision Process (MDP), defined in standard fashion: $\mathcal{M} := \langle \mathcal{S}, \mathcal{A}, \mathcal{R}, P, \gamma, \rho \rangle$. \mathcal{S} and \mathcal{A} denote the state and action space, which we assume are discrete. We use $\mathcal{Z} := \mathcal{S} \times \mathcal{A}$ as the shorthand for the joint state-action space. The reward function $\mathcal{R} : \mathcal{Z} \rightarrow \text{Dist}([0, 1])$ maps state-action pairs to distributions over the unit interval, while the transition function $P : \mathcal{Z} \rightarrow \text{Dist}(\mathcal{S})$ maps state-action pairs to distributions over next states. Finally, $\rho \in \text{Dist}(\mathcal{S})$ is the distribution over initial states. We use \mathbf{r} to denote the expected reward function, $\mathbf{r}(\langle s, a \rangle) := \mathbb{E}_{r \sim \mathcal{R}(\cdot | \langle s, a \rangle)}[r]$, which can also be interpreted as a vector $\mathbf{r} \in \mathbb{R}^{|\mathcal{Z}|}$. Similarly, note that P can be described as $P : (\mathcal{Z} \times \mathcal{S}) \rightarrow \mathbb{R}$, which can be represented as a stochastic matrix $P \in \mathbb{R}^{|\mathcal{Z}| \times |\mathcal{S}|}$.

In order to emphasize that these reward and transition functions correspond to the true environment, we sometimes equivalently denote them as $\mathbf{r}_{\mathcal{M}}, P_{\mathcal{M}}$.

A policy $\pi : \mathcal{S} \rightarrow \Delta(\mathcal{A})$ specifies a conditional distribution over actions given states. A deterministic policy $\mu : \mathcal{S} \rightarrow \mathcal{A}$, which directly selects a single action for each state, can be viewed as a special case of π where the probability of the chosen action is 1 and all others are 0. We denote the space of all possible policies as Π . We define an “activity matrix” for each policy, $A^\pi \in \mathbb{R}^{\mathcal{S} \times \mathcal{Z}}$, which encodes the state-conditional state-action distribution of π , by letting $A^\pi(s, \langle \dot{s}, a \rangle) := \pi(a|s)$ if $s = \dot{s}$, otherwise $A^\pi(s, \langle \dot{s}, a \rangle) := 0$. Acting in the MDP according to π can thus be represented by $A^\pi P \in \mathbb{R}^{|\mathcal{S}| \times |\mathcal{S}|}$ or $PA^\pi \in \mathbb{R}^{|\mathcal{Z}| \times |\mathcal{Z}|}$. We define a value function as any $v : \Pi \rightarrow \mathcal{S} \rightarrow \mathbb{R}$ or $q : \Pi \rightarrow \mathcal{Z} \rightarrow \mathbb{R}$ whose output is bounded by $[0, \frac{R_{\max}}{1-\gamma}]$. We use the shorthand $\mathbf{v}^\pi := \mathbf{v}(\pi)$ and $\mathbf{q}^\pi := \mathbf{q}(\pi)$ to denote the result of applying a value function to a specific policy, which can also be represented as a vector, $\mathbf{v}^\pi \in \mathbb{R}^{|\mathcal{S}|}$ and $\mathbf{q}^\pi \in \mathbb{R}^{|\mathcal{Z}|}$. We use \mathbf{q}^* as the abbreviation of $(\mathbf{q}_{\mathcal{M}}^{\pi^*})^*$, \mathbf{q}_ξ^* as the abbreviation of $(\mathbf{q}_\xi^{\pi_\xi^*})^*$. The terms \mathbf{q} and \mathbf{v} refer to discrete matrix representations, while $Q : \mathbb{R}^{|\mathcal{Z}|} \rightarrow \mathbb{R}$ denotes a more general definition suitable for both discrete and continuous contexts.

To denote the output of an arbitrary value function on an arbitrary policy on a state, we use unadorned $\mathbf{v}(s)$ and $\mathbf{q}(s)$. The *expected return* of an MDP \mathcal{M} , denoted $\rho_{\mathcal{M}}^T \mathbf{v}_{\mathcal{M}}^*$ or $\rho_{\mathcal{M}}^T \mathbf{q}_{\mathcal{M}}^*$, is the discounted sum of rewards starting from initial states, acquired when interacting with the environment:

$$\rho_{\mathcal{M}}^T \mathbf{v}_{\mathcal{M}}^*(\pi) := \rho^T \sum_{t=0}^{\infty} (\gamma A^\pi P)^t A^\pi \mathbf{r} \quad \rho_{\mathcal{M}}^T \mathbf{q}_{\mathcal{M}}^*(\pi) := \rho^T \sum_{t=0}^{\infty} (\gamma P A^\pi)^t \mathbf{r}$$

Note that $(\mathbf{v}_{\mathcal{M}}^\pi)^* = A^\pi (\mathbf{q}_{\mathcal{M}}^\pi)^*$. An *optimal policy* of an MDP, which we denote $\pi_{\mathcal{M}}^*$, is a policy for which the expected return $\mathbf{v}_{\mathcal{M}}$ is maximized under the initial state distribution: $\pi_{\mathcal{M}}^* := \arg \max_{\pi} \mathbb{E}_{\rho}[\mathbf{v}_{\mathcal{M}}^\pi]$. The state-wise expected returns of an optimal policy can be written as $\mathbf{v}_{\mathcal{M}}^{\pi_{\mathcal{M}}^*}$. Of particular interest are value functions whose outputs obey fixed-point relationships, $(\mathbf{v}^\pi)^* = f((\mathbf{v}^\pi)^*)$ for some $f : (\mathcal{S} \rightarrow \mathbb{R}) \rightarrow (\mathcal{S} \rightarrow \mathbb{R})$. The Bellman consistency equation for \mathbf{x} is $\mathcal{B}_{\mathcal{M}}(\mathbf{x}) := \mathbf{r} + \gamma P \mathbf{x}$. Since $(\mathbf{v}_{\mathcal{M}}^{\pi_{\mathcal{M}}^*})^*$ is the only vector for which $(\mathbf{v}_{\mathcal{M}}^{\pi_{\mathcal{M}}^*})^* = A^{\pi_{\mathcal{M}}^*} \mathcal{B}_{\mathcal{M}}((\mathbf{v}_{\mathcal{M}}^{\pi_{\mathcal{M}}^*})^*)$

holds. Finally, for any state s , the probability of being in the state s' after t time steps when following policy π is $[(A^\pi P)^t](s, s')$. Furthermore, $\sum_{t=0}^{\infty} (\gamma A^\pi P)^t = (I - \gamma A^\pi P)^{-1}$. We refer to $\frac{1}{1-\gamma} (I - \gamma A^\pi P)^{-1}$ as the discounted visitation of π .

Datasets. We begin by defining fundamental concepts essential for addressing the challenge of fixed-dataset policy optimization. We define a dataset D consisting of d transitions as $D := \langle s, a, r, s' \rangle^d$ and denote the set of all such datasets as \mathcal{D} . Our focus is on datasets sampled from a data distribution $\Phi : \text{Dist}(\mathcal{Z})$, typically derived from the state-action pairs generated under a stationary policy. We represent the construction of a dataset containing d tuples $\langle s, a, r, s' \rangle$ by $D \sim \Phi_d$, where each pair $\langle s, a \rangle$ is sampled from Φ , and the rewards r and subsequent states s' are sampled iid from the reward function $\mathcal{R}(\cdot | \langle s, a \rangle)$ and the transition function $P(\cdot | \langle s, a \rangle)$, respectively.

³ We sometimes index D using function notation, using $D(s, a)$ to denote the multi-set of all $\langle r, s' \rangle$ such that $\langle s, a, r, s' \rangle \in D$. We use $\ddot{\mathbf{n}}_D \in \mathbb{R}^{|\mathcal{Z}|}$ to denote the vectors of counts, that is, $\ddot{\mathbf{n}}_D(\langle s, a \rangle) := |D(s, a)|$. We sometimes use state-wise versions of these vectors, which we denote with $\dot{\mathbf{n}}_D$. It is further useful to consider the maximum-likelihood reward and transition functions, computed by averaging all rewards and transitions observed in the dataset for each state-action. To this end, we define empirical reward vector $\mathbf{r}_D(\langle s, a \rangle) := \sum_{r, s' \in D(\langle s, a \rangle)} \frac{r}{|D(\langle s, a \rangle)|}$ and empirical transition matrix $P_D(s' | \langle s, a \rangle) := \sum_{r, s' \in D(\langle s, a \rangle)} \frac{\mathbb{I}(s'=s')}{|D(\langle s, a \rangle)|}$ at all state-actions for which $\ddot{\mathbf{n}}_D(\langle s, a \rangle) > 0$. Where with $\ddot{\mathbf{n}}_D(\langle s, a \rangle) = 0$, there is no clear way to define the maximum-likelihood estimates of reward and transition, so we do not specify them. All our results hold no matter how these values are chosen, so long as $\mathbf{r}_D \in [0, \frac{R_{\max}}{1-\gamma}]$ and P_D is stochastic. The empirical policy of a dataset D is defined as $\hat{\pi}_D(a|s) := \frac{|D(\langle s, a \rangle)|}{|D(\langle s, \cdot \rangle)|}$ except where $\ddot{\mathbf{n}}_D(\langle s, a \rangle) = 0$, where it can similarly be any valid action distribution. The empirical visitation distribution of a dataset D is computed in the same way as the visitation distribution, but with P_D replacing P , i.e. $\frac{1}{1-\gamma} (I - \gamma A^\pi P_D)^{-1}$.

B Proofs

Lemma 1. *For any MDP ξ and policy π , consider the Bellman fixed-point equation given by, let $(\mathbf{v}_\xi^\pi)^*$ be defined as the unique value vector such that $(\mathbf{v}_\xi^\pi)^* = A^\pi(\mathbf{r}_\xi + \gamma P_\xi(\mathbf{v}_\xi^\pi)^*)$, and let \mathbf{v} be any other value vector. Assume that $\pi(a|s) = 1$ if $a = \arg \max_a (\mathbf{q}_\xi^\pi)^*(s, a)$, otherwise $\pi(a|s) = 0$. We have:*

$$|\mathbf{q}_\xi^*(s, \mu(s)) - \mathbf{q}(s, \mu(s))| = |((I - \gamma A^\pi P_\xi)^{-1}(A^\pi(\mathbf{r}_\xi + \gamma P_\xi \mathbf{v}) - \mathbf{v}))(s)| \quad (4)$$

Proof.

$$\begin{aligned} A^\pi(\mathbf{r}_\xi + \gamma P_\xi \mathbf{v}) - \mathbf{v} &= A^\pi(\mathbf{r}_\xi + \gamma P_\xi \mathbf{v}) - (\mathbf{v}_\xi^\pi)^* + (\mathbf{v}_\xi^\pi)^* - \mathbf{v} \\ &= A^\pi(\mathbf{r}_\xi + \gamma P_\xi \mathbf{v}) - A^\pi(\mathbf{r}_\xi + \gamma P_\xi (\mathbf{v}_\xi^\pi)^*) + (\mathbf{v}_\xi^\pi)^* - \mathbf{v} \\ &= \gamma A^\pi P_\xi(\mathbf{v} - (\mathbf{v}_\xi^\pi)^*) + ((\mathbf{v}_\xi^\pi)^* - \mathbf{v}) \\ &= ((\mathbf{v}_\xi^\pi)^* - \mathbf{v}) - \gamma A^\pi P_\xi((\mathbf{v}_\xi^\pi)^* - \mathbf{v}) \\ &= (I - \gamma A^\pi P_\xi)((\mathbf{v}_\xi^\pi)^* - \mathbf{v}) \end{aligned}$$

Note that $(\mathbf{v}_\xi^\pi)^* = A^\pi(\mathbf{q}_\xi^\pi)^*$, After we expand the value function we have:

$$\begin{aligned} (I - \gamma A^\pi P_\xi)^{-1}(A^\pi(\mathbf{r}_\xi + \gamma P_\xi \mathbf{v})) &= A^\pi(\mathbf{q}_\xi^\pi)^* - \mathbf{v} \\ &= A^\pi(\mathbf{q}_\xi^\pi)^* - A\mathbf{q} \end{aligned}$$

by indexing $\langle s, \mu(s) \rangle$, we have:

$$|\mathbf{q}_\xi^*(s, \mu(s)) - \mathbf{q}(s, \mu(s))| = |((I - \gamma A^\pi P_\xi)^{-1}(A^\pi(\mathbf{r}_\xi + \gamma P_\xi \mathbf{v}) - \mathbf{v}))(s)|$$

□

³Note that this is in some sense a simplifying assumption. In practice, it is common to collect data sets using trajectories of non-stationary policies rather than i.i.d. This assumption facilitates our derivation of the previous term.

B.1 Proof of Theorem 1

Note that \mathbf{q} is the matrix representation of the Q function. In the proof of this section, we use a more general $Q : \mathbb{R}^Z \rightarrow \mathbb{R}$ to represent the Q function. The update formula for \hat{Q} iteration is:

$$\hat{Q}^{k+1}(s, a) = (1 - \alpha)\hat{Q}^k(s, a) + \alpha \left(r(s, a) + \gamma \sum_{s' \in S} P(s'|s, a) \max_a \hat{Q}(s', a) \right)$$

And the update formula can be defined as **Bellman optimal operator \mathcal{B}** :

$$\hat{Q}^*(s, a) = \mathcal{B}\hat{Q}^* = r(s, a) + \gamma \sum_{s' \in S} P(s'|s, a) \max_a \hat{Q}^*(s', a)$$

Next we prove that the Bellman optimal operator \mathcal{B} is γ -contraction operator on \hat{Q} :

$$\begin{aligned} \|\mathcal{B}\hat{Q} - \mathcal{B}\hat{Q}'\|_\infty &= \gamma \max_{s, a \in S, \mathcal{A}} \left| \sum_{s'} P(s'|s, a) [\max_a \hat{Q}(s', a) - \max_a \hat{Q}'(s', a)] \right| \\ &\leq \gamma \max_{s, a \in S, \mathcal{A}} \left| \max_{s'} \left(\max_a \hat{Q}(s', a) - \max_a \hat{Q}'(s', a) \right) \right| \\ &= \gamma \|\hat{Q} - \hat{Q}'\|_\infty \end{aligned}$$

The Bellman optimal operator \mathcal{B} is a γ -contraction operator on \hat{Q} , which means that as the number of iteration k continues to increase, \hat{Q}^k will get closer to the fixed point, i.e., \hat{Q}^* . Next, we prove that the converged heuristic-guided Q function equals the traditional Q function. Define the following:

Θ_H denotes the set of terminal states,

Θ_{H-1} denotes the set of states one step before the terminal,

\vdots

Θ_1 denotes the set of states at the initial step.

For $s \in \Theta_{H-1}$, it's clear that $\hat{Q}^*(s) = Q^*(s)$, because:

$$Q^*(s, a)|_{s \in \Theta_{H-1}} = \hat{Q}^*(s, a)|_{s \in \Theta_{H-1}} = r(s, a) + \gamma Q^*(s') = r(s, a)$$

For $s \in \Theta_{H-2}$, which is the previous state in Θ_{H-1} , we have:

$$\begin{aligned} \hat{Q}^*(s, a)|_{s \in \Theta_{H-2}} &= r(s, a) + \gamma \sum_{s' \in \Theta_{H-1}} P(s'|s, a) \hat{Q}^*(s') \\ &= r(s, a) + \gamma \sum_{s' \in \Theta_{H-1}} P(s'|s, a) Q^*(s') \\ &= Q^*(s, a)|_{s \in \Theta_{H-2}} \end{aligned}$$

With constant iteration, we have: $\hat{Q}^* = Q^*$. Specifically, we have: $\mathbf{q}_D = \hat{\mathbf{q}}_D$

B.2 Proof of Suboptimality

$$\begin{aligned} (\mathbf{q}^{\pi^*})^*(s, a^{\pi^*}) - (\hat{\mathbf{q}}^{\pi^*})^*(s, a^{\pi^*}) &= (\mathbf{q}^{\pi^*})^*(s, a^*) + [-(\hat{\mathbf{q}}_D^{\pi^*})^*(s, a^{\pi^*}) + (\hat{\mathbf{q}}_D^{\pi^*})^*(s, a^{\pi^*})] + \\ &\quad [-(\hat{\mathbf{q}}_D^{\pi^*})^*(s, a^{\pi^*}) + (\hat{\mathbf{q}}_D^{\pi^*})^*(s, a^{\pi^*})] - (\mathbf{q}^{\pi^*})^*(s, a^{\pi^*}) \\ &= [(\mathbf{q}^{\pi^*})^*(s, a^*) - (\hat{\mathbf{q}}_D^{\pi^*})^*(s, a^{\pi^*})] + [(\hat{\mathbf{q}}_D^{\pi^*})^*(s, a^{\pi^*}) - (\hat{\mathbf{q}}_D^{\pi^*})^*(s, a^{\pi^*})] \\ &\quad + [(\hat{\mathbf{q}}_D^{\pi^*})^*(s, a^{\pi^*}) - (\mathbf{q}^{\pi^*})^*(s, a^{\pi^*})] \\ &\leq [(\mathbf{q}^{\pi^*})^*(s, a^*) - (\hat{\mathbf{q}}_D^{\pi^*})^*(s, a^{\pi^*})] + [(\hat{\mathbf{q}}_D^{\pi^*})^*(s, a^{\pi^*}) - (\mathbf{q}^{\pi^*})^*(s, a^{\pi^*})] \end{aligned}$$

We treat the RHS as a function of π , so we have:

$$\begin{aligned}
(\mathbf{q}^{\pi^*})^*(s, a^{\pi^*}) - (\mathbf{q}^{\pi_D^*})^*(s, a^{\pi_D^*}) &\leq \inf_{\pi \in \Pi} ([(\mathbf{q}^{\pi^*})^*(s, a^*) - (\hat{\mathbf{q}}_D^\pi)^*(s, a^\pi)] + [(\hat{\mathbf{q}}_D^{\pi_D^*})^*(s, a^{\pi_D^*}) - (\mathbf{q}^{\pi_D^*})^*(s, a^{\pi_D^*})]) \\
&\leq \inf_{\pi \in \Pi} ((\mathbf{q}^{\pi^*})^*(s, a^*) - (\hat{\mathbf{q}}_D^\pi)^*(s, a^\pi)) + \sup_{\pi \in \Pi} ((\hat{\mathbf{q}}_D^\pi)^*(s, a^\pi) - (\mathbf{q}^{\pi^*})^*(s, a^\pi)) \\
&= \inf_{\pi \in \Pi} ((\mathbf{q}^{\pi^*})^*(s, a^*) - (\mathbf{q}_D^{\pi_D^*})^*(s, a^{\pi_D^*}) + (\mathbf{q}_D^{\pi_D^*})^*(s, a^{\pi_D^*}) + (\hat{\mathbf{q}}_D^\pi)^*(s, a^\pi)) \\
&\quad + \sup_{\pi \in \Pi} ((\hat{\mathbf{q}}_D^\pi)^*(s, a^\pi) - (\mathbf{q}^{\pi^*})^*(s, a^\pi))
\end{aligned}$$

B.3 Proof of Theorem 2

First, we consider the simplest possible bound. \mathbf{v}^* and \mathbf{q}^* are bounded in $[0, \frac{R_{\max}}{1-\gamma}]$, so both $A^\pi(\mathbf{r}_M + \gamma P_M \mathbf{v})$ and $A^\pi(\mathbf{r}_D + \gamma P_D \mathbf{v})$ must be as well. Thus, their difference is also bounded:

$$|A^\pi(\mathbf{r}_M + \gamma P_M \mathbf{v}) - A^\pi(\mathbf{r}_D + \gamma P_D \mathbf{v})| \leq \frac{R_{\max}}{1-\gamma}$$

Next, consider that for any $\langle s, a \rangle$, the expression $\mathbf{r}_D(\langle s, a \rangle) + \gamma P_D(\langle s, a \rangle) \mathbf{v}^\pi$ can be equivalently expressed as an expectation of random variables,

$$\mathbf{r}_D(\langle s, a \rangle) + \gamma P_D(\langle s, a \rangle) \mathbf{v} = \frac{1}{\ddot{\mathbf{n}}_D(\langle s, a \rangle)} \sum_{r, s' \in D(\langle s, a \rangle)} r + \gamma \mathbf{v}(s')$$

each with expected value:

$$\mathbb{E}_{r, s' \in D(\langle s, a \rangle)} [r + \gamma \mathbf{v}(s')] = \mathbb{E}_{\substack{r \sim \mathcal{R}(\cdot | \langle s, a \rangle) \\ s' \sim P(\cdot | \langle s, a \rangle)}} [r + \gamma \mathbf{v}(s')] = [\mathbf{r}_M + \gamma P_M \mathbf{v}](\langle s, a \rangle).$$

Hoeffding's inequality indicates that the mean of bounded random variables will approximate their expected values with high probability. By applying Hoeffding's inequality to each element in the $|\mathcal{S} \times \mathcal{A}|$ state-action space and employing a union bound, we establish that with probability at least $1 - \delta$,

$$|(\mathbf{r}_M + \gamma P_M \mathbf{v}) - (\mathbf{r}_D + \gamma P_D \mathbf{v})| \leq \frac{1}{1-\gamma} \sqrt{\frac{1}{2} \ln \frac{2|\mathcal{S} \times \mathcal{A}|}{\delta}} \ddot{\mathbf{n}}_D^{-1}$$

We can left-multiply A^π and rearrange to get:

$$|A^\pi(\mathbf{r}_M + \gamma P_M \mathbf{v}) - A^\pi(\mathbf{r}_D + \gamma P_D \mathbf{v})| \leq \left(\frac{1}{1-\gamma} \sqrt{\frac{1}{2} \ln \frac{2|\mathcal{S} \times \mathcal{A}|}{\delta}} \right) A^\pi \ddot{\mathbf{n}}_D^{-\frac{1}{2}}$$

then we left-multiply the discounted visitation of π :

$$|(I - \gamma A^\pi P_D)^{-1} [A^\pi(\mathbf{r}_M + \gamma P_M \mathbf{v}) - A^\pi(\mathbf{r}_D + \gamma P_D \mathbf{v})]| \leq \left(\frac{1}{1-\gamma} \sqrt{\frac{1}{2} \ln \frac{2|\mathcal{S} \times \mathcal{A}|}{\delta}} \right) (I - \gamma A^\pi P_D)^{-1} A^\pi \ddot{\mathbf{n}}_D^{-\frac{1}{2}}$$

This matrix: $(I - \gamma A^\pi P_D)^{-1} A^\pi \ddot{\mathbf{n}}_D^{-\frac{1}{2}}$, is of dimension $\mathbb{R}^{|\mathcal{S}|}$:

$$(I - \gamma A^\pi P_D)^{-1} A^\pi \ddot{\mathbf{n}}_D^{-\frac{1}{2}}(s) = (1-\gamma) \sum_{s'} \nu(s' | s_0 = s) \frac{1}{\sqrt{N_D(\langle s, \mu(s) \rangle)}}$$

Finally, to integrate these term together we have the bound on theorem 2:

$$|\mathbf{q}_D^*(s) - \mathbf{q}^*(s)| \leq \left(\sqrt{\frac{1}{2} \ln \frac{2|\mathcal{S} \times \mathcal{A}|}{\delta}} \right) \sum_{s'} \nu(s' | s_0 = s) \frac{1}{\sqrt{N_D(\langle s', \mu(s') \rangle)}}$$

B.4 Proof of Theorem 3

To get the sample complexity of convergence. By 2, we have:

$$\begin{aligned}
|\mathbf{q}_D^*(s) - \mathbf{q}^*(s)| &\leq \left(\sqrt{\frac{1}{2} \ln \frac{2|\mathcal{S} \times \mathcal{A}|}{\delta}} \right) \sum_{s'} \nu(s'|s_0 = s) \frac{1}{\sqrt{N_D(\langle s', \mu(s') \rangle)}} \\
&= C \sum_{s'} \sqrt{\nu(s'|s_0 = s)} \frac{\sqrt{\nu(s'|s_0 = s)}}{\sqrt{nd_D(s, a)}} \quad (d_D(s, a) = \frac{N_D(\langle s, a \rangle)}{|D|}) \\
&= C \sum_{s'} \sqrt{d_D(s, \mu(s))} \frac{\sqrt{d_D(s, \mu(s))}}{\sqrt{nd_D(s, a)}} \quad (\nu(s)\pi(\mu(s)|s) \approx d_D(s, \mu(s))) \\
&\leq \frac{C}{\sqrt{n}} \sum_{s'} \sqrt{d_D(s', \mu(s))} \\
&\leq \left(\sqrt{\frac{1}{2} \ln \frac{2|\mathcal{S} \times \mathcal{A}|}{\delta}} \right) \frac{|S|}{\sqrt{n}}
\end{aligned}$$

Then, when $n > \mathcal{O}\left(\frac{|S|^2}{2\epsilon^2} \ln \frac{2|\mathcal{S} \times \mathcal{A}|}{\delta}\right)$, we have $|\mathbf{q}_D^*(s, \mu(s)) - \mathbf{q}^*(s, \mu(s))| \leq \epsilon$.

C Online-Guidance Implementation

Algorithm 2 Online Heuristic Q Learning Algorithm

- 1: **Inputs:** Local MDP D , Large Language Model G , prompt p ,
 - 2: **Initialization:** Initialize Heuristic: $G(p)$, initialize actor-critic $(\mu_\phi, Q_{\theta_1}, Q_{\theta_2})$ and target actor-critic $(\mu_{\phi'}, Q_{\theta'_1}, Q_{\theta'_2})$
 - 3: **Generate Q buffer:** $D_g \leftarrow \{(s_i, a_i, Q_i) \mid (s_i, a_i, Q_i) = G(p), i = 1, 2, \dots, n\}$
 - 4: **Q Bootstrapping:** $\theta = \theta - \alpha \nabla_{\theta} L_{bootstrap}$ using eq 2
 - 5: **for** iteration $t' \in T = 1, 2, 3, \dots$ **do**
 - 6: Sample (s, a, r, s') from Env
 - 7: $D \leftarrow D \cup (s, a, r, s')$
 - 8: Sample N transitions (s, a, r, s') from D
 - 9: **Detect interaction:** $D_g = \begin{cases} D(G(p, t')) & \text{if detected} \\ \text{null} & \text{if not} \end{cases}$
 - 10: $\hat{a} \leftarrow \mu(s') + \epsilon, \epsilon \sim \text{clip}(\mathcal{N}(0, \sigma), -c, c)$
 - 11: $y(s') \leftarrow \lceil r + \gamma \min_{i=1,2} \mathbf{q}_{\theta_i}(s', \hat{a}) \rceil$
 - 12: Update critics $\theta_i \leftarrow \arg \min_{\theta_i} L_{online}(\theta_i)$
 - 13: **if** $t' \bmod d$ **then**
 - 14: Update actor $\phi \leftarrow \arg \min_{\phi} L_{actor}(\phi)$
 - 15: Update target networks:
 - 16: $\theta'_i \leftarrow \tau \theta_i + (1 - \tau) \theta'_i$
 - 17: $\phi' \leftarrow \tau \phi + (1 - \tau) \phi'$
 - 18: **end if**
 - 19: **end for**
 - 20: **end while**
-

D Prompt